

# SEISMIC BEHAVIOR OF CIRCULAR FLY ASH CONCRETE COLUMN REINFORCED BY ULTRA HIGH STRENGTH REBARS AND STEEL PLATES

Junhua WANG<sup>\*1</sup>, Takashi TAKEUCHI<sup>\*2</sup>, Tomoyuki KOYAMA<sup>\*3</sup>, Yuping SUN<sup>\*4</sup>

## ABSTRACT

This paper experimentally studied influences of the types of longitudinal rebars and transverse reinforcement methods on seismic behavior of circular fly ash concrete column. The experimental results have indicated that specimens with high strength rebars having low bond strength exhibit smaller residual deformation and more stable resistance than that of the specimens with high-strength deformed rebars. The specimens confined by steel plates showed not only higher lateral resistance but also less residual deformation than the specimens confined by conventional spirals.

Keyword: Fly ash concrete column, Residual deformation, Ultra-high strength steel, Steel plate

## 1 INTRODUCTION

Sustainability has been one of the key words for building and civil structures in the 21<sup>st</sup> century. Numerous studies have been conducted in recent decades to develop sustainable materials, for example, Matsufuji et al.[1,2] have proposed the use of fine fly-ash in concrete structure rather as partial replacement of fine aggregate than as conventional replacement of cement, and experimentally verified that this application of fine fly-ash could increase not merely compressive strength of concrete but also durability due to improvement in bonding property of mortar paste. The point of the method by Matsufuji et al. to utilize fine fly-ash lies in that it can reduce the amount of cement and river sand simultaneously, while providing higher strength and sounder durability, and contribute to significantly mitigating environmental burden of concrete industry.

Resilience is another key word and means capacity to return to origin state. The lessons learnt from substantial damages caused by mega-earthquakes such as 5.12 Sichuan Earthquake in 2008 and 3.11 Eastern Japan Earthquake in 2011 have taught human society importance of seismic resilience of infra and building structures from the viewpoint of prompt recovery and reconstruction of society after earthquakes.

Sun et al have recently proposed a simple method to make resilient concrete structures [3]. This method only involves the use of ultra-high strength rebar with low bond strength. The SBPDN 1275/1420 rebar, which has spiral groove on its surface and has been adopted in Japan mainly as transverse reinforcement of high strength concrete members, is used as longitudinal rebars of the resilient concrete components proposed by

Sun et al.

Until now, Sun et al. have conducted experimental study on seismic behavior of prismatic concrete columns reinforced by the SBPDN 1275/1420 rebar and verified that use of the SBPDN 1275/1420 rebar could assure concrete columns stable response up to 0.04rad. only if the rebars were mechanically fixed at both ends[4]. Purposes of this study are to present experimental information on seismic behavior of circular fly-ash concrete columns and to investigate effectiveness of the SBPDN 1275/1420 rebars on resilience when combined with high-strength concrete. Since the use of a large quantity of fine fly-ash in partial replacement of fine aggregate leads to higher concrete strength, finding of effective confinement method for high-strength concrete is another research item of this study.

## 2 EXPERIMENTAL PROGRAM

### 2.1 Outlines of Test Columns

Four circular specimens were fabricated and tested under combined constant axial compression and reversed lateral load. As shown in Fig.1, the diameter and shear span are 250mm and 500mm, respectively. Fly ash concrete was used to cast the columns with target strength of 80MPa. The experimental variables were the type of longitudinal rebars and the confinement method of column. The specimens were divided into two groups, SB and US, according to the type of longitudinal rebars used. SB series specimens were reinforced by eight SBPDN 1275/1420 rebars, while US series specimens were reinforced by eight deformed USD 685 rebars. Specimens FANSB and FANUS were confined with D6 spirals, and specimens

\*1 Graduate Student, Graduate School of Engineering, Kobe University, JCI Student Member

\*2 Assistant Professor, Graduate School of Engineering, Kobe University, JCI Member

\*3 Associate Professor, Faculty of Human-Environment Studies, Kyushu University, JCI Member

\*4 Professor, Graduate School of Engineering, Kobe University, JCI Member

FATSB and FATUS were confined with individual circular D6 hoops and steel plates with height of 1.4D (D is the diameter of column section). Each specimen was under constant axial compression ratio of 0.3. Due to the limitation of capacity in laboratory, of the total the axial compression of 1200kN, approximately 400kN was provided by a PC bar as shown in Fig.1. The outlines of the test specimens are summarized in Table1.

## 2.2 Material Properties

Ready-mix concrete was used to fabricate the specimens. Table 2 shows details of mix proportion of the concrete. As seen from Table 2, up to 455kg of fine fly-ash was used to replace fine aggregate in per cubic meter. The specimens were cured in the forms with their tops covered by wet burlaps for four weeks after casting and then were air-cured after removal of the forms. The concrete strengths at the test age were given in Table 1.

Fig.2 and Table 3 show tensile stress-strain curves and mechanical properties of the steels used, respectively. The SBPDN 1275/1420 rebar has yield strength of 1423MPa and 12.6 mm in diameter while the USD D13 deformed rebar has yield strength of 961MPa. The thickness of steel plate used to constrain concrete is 3.2mm, and its yield strength is 325MPa.

## 2.3 Test Setup and Loading Program

All columns were tested under simultaneously applied axial compression and lateral displacement reversals. Fig.3 illustrates the test setup which consisted of a steel loading beam assembly, a 300kN hydraulic jack and a 1000kN capacity hydraulic jack. The 1000kN capacity hydraulic jack was used to apply

the constant axial compression throughout the test, and cyclically reversed lateral load was applied by the 300kN hydraulic jack.

Lateral load was controlled by drift ratio(R), which is defined as the ratio of the tip lateral displacement to the shear span of the column. The lateral displacement history consisted of incrementally increasing deformation reversals. Two complete cycles were applied at each level of lateral displacement when R reached 0.02rad., and only one cycle was applied at each level of lateral displacement when R become larger than 0.02rad.. Due to the ultimate capacities of specimen FATSB and FATUS exceeded the loading capacity of the hydraulic jack in pull direction. These two specimens were deformed only up to 0.03 rad. and 0.02 rad. in pull direction.

One displacement transducer (DT) was installed to measure the tip lateral displacement, and four DTs were used to measure the axial displacement of each column. Eight strain gages were tied to measure the axial strain of two longitudinal rebars located at the tensile and compressive sides, and six strain gages were attached at the transverse reinforcement. The strain gages were located at the sections 25mm, 145mm, 245mm away from the loading stub, respectively.

The steel plates used to confine the column consist of two pieces of half circular steel plates closed by two batches of bolts along the web sides of column. Six strain gages were tied on the surface of steel plates to measure the strains of horizontal and vertical strains. In order for the steel plates to avoid direct resisting to the axial stress by axial compression and bending moment, clearance of 6mm was provided between the lower end of steel plates and the loading stub.

Table 1 Properties of specimens

Specimen	$f'_c$ (N/mm <sup>2</sup> )	Longitudinal rebar		Transverse reinforcement					$Q_{exp}$ (kN)	$R_{expQ}$ (0.01rad.)
		Name	$\rho_g$ (%)	$s$ (mm)	$\rho_h$ (%)	Steel plate	$t$ (mm)	$\rho_t$ (%)		
FANSB	78.7	SBPDN rebar	2.05	30	1.98	No	-	-	230	3.0
FATSB	78.7			90	0.66	Yes	3.2	2.5	313	5.0
FANUS	76.8	USD rebar	2.07	30	1.98	No	-	-	261	2.5
FATUS	73.8			90	0.66	Yes	3.2	2.5	318	3.0

Note:  $f'_c$ =concrete compression strength;  $\rho_g$ = the ratio of longitudinal rebar;  $s$ =the spacing of transverse reinforcement;  $\rho_h$ =the volumetric ratio of spirals;  $Q_{exp}$ = Ultimate lateral load;  $R_{expQ}$ = drift angle at  $Q_{exp}$ ;  $t$ =thickness of steel plate;  $\rho_t$ = the volumetric ratio of steel plate.

Table 2 Mix proportion of concrete

Fly Ash (kg/m <sup>3</sup> )	W/C	Water (kg/m <sup>3</sup> )	Cement (kg/m <sup>3</sup> )	Fine Aggregate		Coarse Aggregate (kg/m <sup>3</sup> )	Admixture (kg/m <sup>3</sup> )
				Sand (kg/m <sup>3</sup> )	Crushed Sand (kg/m <sup>3</sup> )		
455	0.65	185	285	334	146	833	5.92

Table 3 Mechanical properties of the steels

Name	Type	$f_y$ (N/mm <sup>2</sup> )	$f_u$ (N/mm <sup>2</sup> )	$E_s$ (N/mm <sup>2</sup> )	$\varepsilon$ (%)
SBPDN rebars	SBPDN 1275/1420	1423**	1499	215000	0.86**
USD rebars	USD 685*	961**	1037	182000	0.72**
PL3.2	SS400	325**	503	194000	0.37**
D6	SD295	426	517	190000	0.23

Note:  $f_y$ =yield stress;  $f_u$ =ultimate stress;  $E_s$ = young modulus;  $\varepsilon$ = yield strain; USD685\* is hardening strength;  $\varepsilon=0.37\%^{**}$ ,  $\varepsilon=0.86\%^{**}$  are obtained according to the 0.2% offset method.

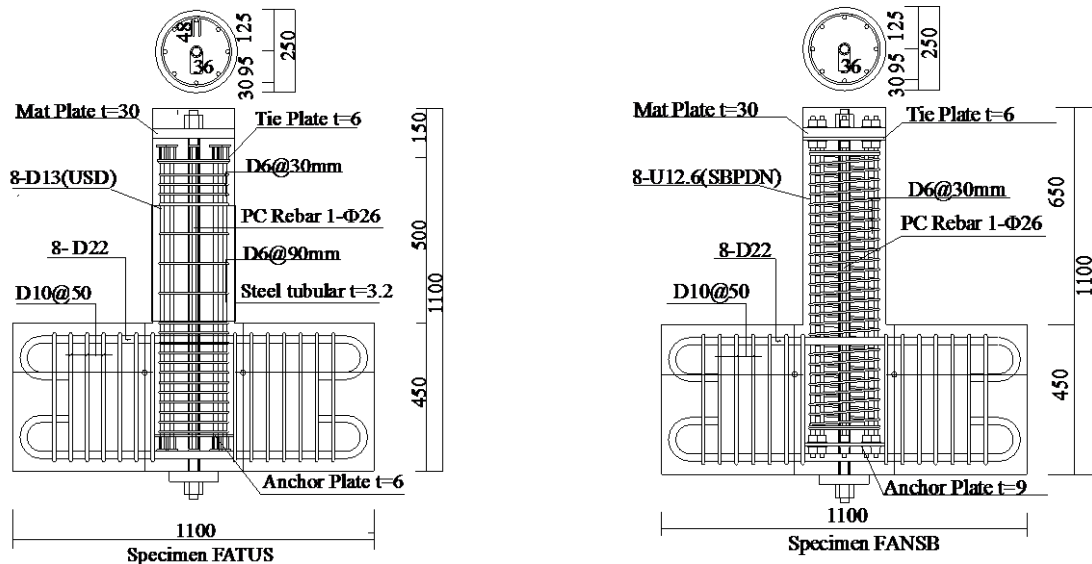


Fig.1 Reinforcement details of the specimens (unit: mm)

### 3 EXPERIMENTAL RESULTS AND DISCUSSIONS

#### 3.1 Observed ultimate patterns

For specimen FANUS, the flexural crack appeared when  $R$  was 0.0025rad., and some shear cracks occurred and connected to the flexural cracks as  $R$  was 0.0075rad., then the axial bond-splitting cracks appeared at the bottom of both sides of column while  $R$  reached -0.01rad.. As  $R$  was beyond 0.015rad., shear cracks spread further, more axial bond-splitting cracks spread upward, and the concrete shell began to spall off. Until  $R$  reached -0.025rad., shear cracks have hardly spread, and too much cover concrete continued spalling off. The first flexural crack was observed in specimen FANSB when  $R$  was 0.0025rad., and the flexural cracks began to diagonally downward spread as  $R$  was 0.005rad.. Axial cracks appeared while  $R$  was -0.0075rad. and cover concrete began to spall off. As  $R$  was 0.015rad., shear cracks have sufficiently spread along the height of column and development of the shear cracks couldn't be seen further, because the massive concrete had spalled off within the 1.5D critical regions of the column from the column bottom. After that deformation level, however, the axial bond-splitting cracks still continued to spread upward.

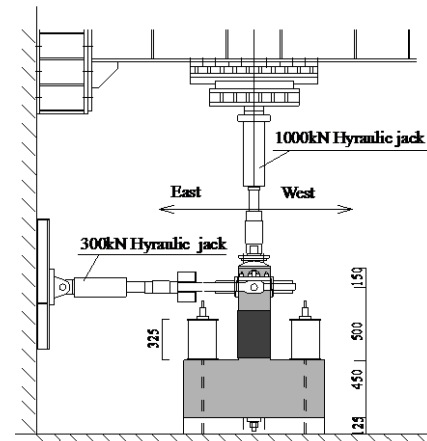


Fig.3 Schematic view of test setup(unit:mm)

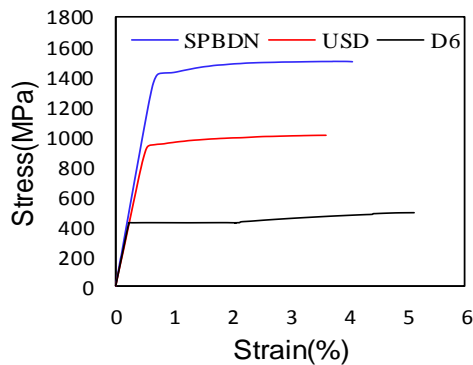


Fig.2. Stress-strain relationships of rebars

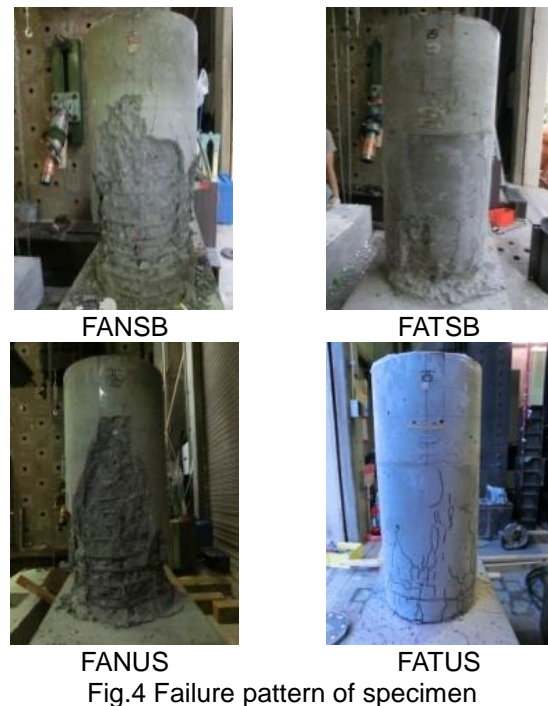


Fig.4 Failure pattern of specimen

Fig.4 shows ultimate patterns of the specimens. The ultimate patterns of specimens confined by steel plates were observed by removing the steel plates after testing. From Fig.4 we can see that the damage of specimens confined by steel plates is much slighter than that of specimen confined by traditional spirals.

### 3.2 Lateral load – drift angle hysteretic responses

The lateral load – drift angle hysteretic responses of all specimens are shown as Fig.5, the solid circles and squares superimposed in Fig.5 represent the cracking load and the ultimate load of each column, respectively. While the dotted line represents the so-called P- $\delta$  mechanism line.

The cracking load of specimen FANUS in push and pull direction are 110kN and -105kN, respectively. While the cracking loads of specimen FANSB in push and pull directions are 113kN and -90kN, respectively.

The envelop curves of the moment versus drift angle relationship were compared in Fig.6, which only displays the moment envelop curves in the positive direction due to the lack of data in negative direction because the resistance of specimens FATSFB and FATUS exceeded the loading capacity of the hydraulic jack in negative direction.

As apparent from Fig.5 and Fig.6, the lateral resistances of the specimens with SBPDN 1275/1420 rebars stably increased up to such a large deformation level as R reached 0.035rad. and 0.05rad., respectively. Degradation in lateral resistance occurred in specimen FANSB after R exceeded 0.035rad., along with

spreading of spalling-off of the cover concrete, but the decline slope was less than the P- $\delta$  effect. On the other hand, the specimens made of USD685 rebar exhibited stable increase till R reached 0.025rad. and 0.03rad., respectively.

Though sharp drop in lateral resistance of specimen FANUS was observed after the peak point, the specimen still remained its axial load sustaining capacity till end of the test at R =0.05rad..

One can also see from Fig.6 that confinement by thin steel plates enhanced the post-peak capacity significantly, which implies that the steel plate confinement could improve greatly the inherent brittleness of high strength concrete. In addition to enhancement effect on ductility of concrete, it is noteworthy from Table 4 that confinement by steel plate can simultaneously increase lateral load resisting capacity of fly-ash concrete column. As compared with the lateral resistance of specimens confined by spirals, the increment in lateral load capacity of the specimens confined by steel plates varied from about 10% at R=0.01rad. up to about 40% at R=0.03rad..

Table 4 Lateral load at every cyclic drift angle R(%)

Notation	$Q_{exp}(kN)$				
	R=1	R=2	R=3	R=4	R=5
FANSB	204	223	230	226	199
FATSFB	235	276	304	302	313
FANUS	220	256	220	180	120
FATUS	245	309	318	309	305

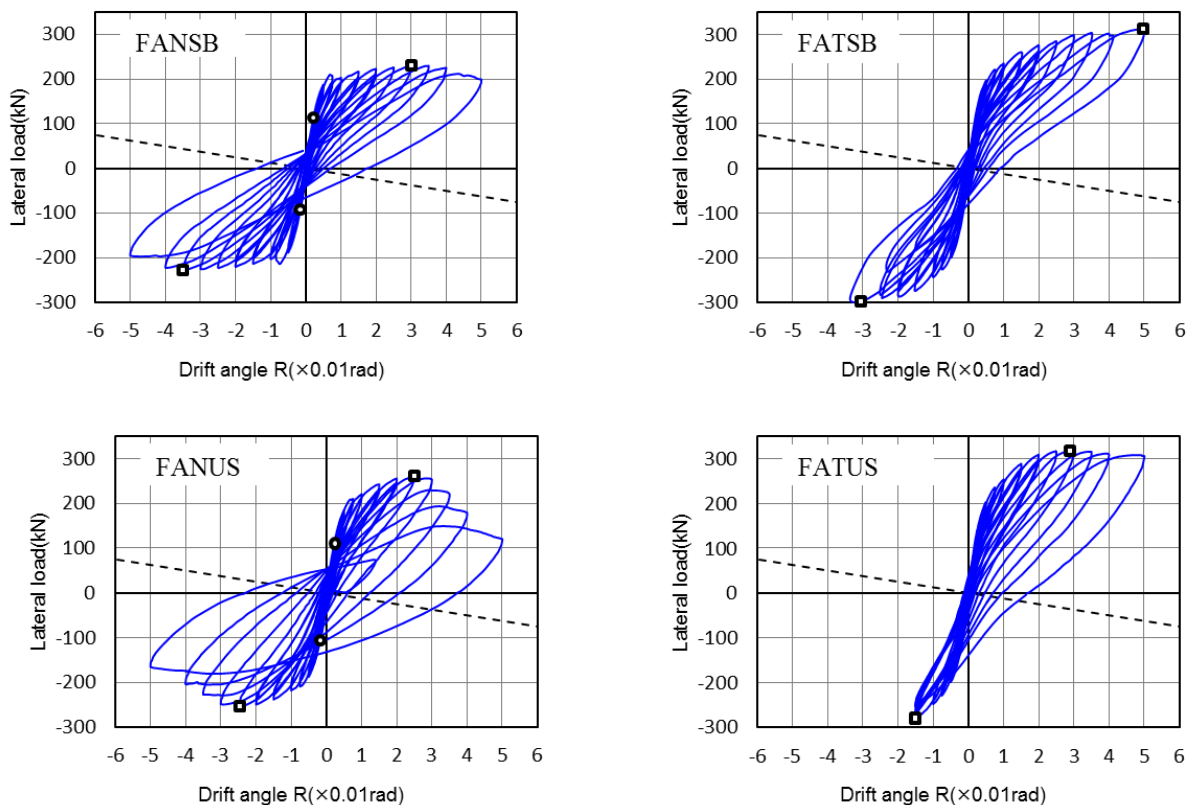


Fig.5 Lateral load versus drift ratio relationship

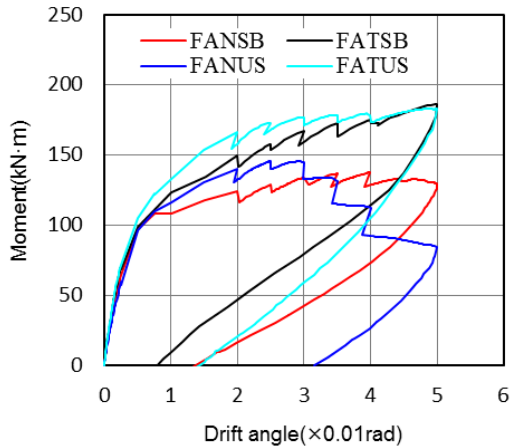


Fig.6 Envelop curves of moment – drift angle

### 3.3 Strains measured in longitudinal rebars

To investigate the reason for the stable increment in lateral resistance observed in the specimens reinforced by ultra-high strength SBPDN 1275/1420 rebars, Fig.7 plots strains of longitudinal rebars measured at the section 25mm away from the column bottom. The blue lines and red lines represent the strain at initially tensile and compressive side, respectively. The black dotted line expressed the yield strain of the longitudinal rebars.

The strains of SBPDN rebars increased by the same rate as that of strains measured in USD rebars till  $R=0.0075\text{rad.}$ , but the increment rate became less than that of USD rebars after  $R=0.0075\text{rad.}$ , which implies that the SBPDN rebars began to slip from that deformation level on. The SBPDN rebars didn't reach its yield strain in tension till  $R=0.05\text{rad.}$  The SBPDN

rebars in specimen FANSB reached its yield strain in compression at  $R=0.04\text{rad.}$ , because of the severe spalling-off of the concrete shell. The stable increase in tensile strain contributed to the stable increase in lateral resistance of column till large deformation. For the specimens with USD rebars, however, the tensile strains reached its yield strain at about  $R=0.03\text{rad.}$ , and from then on, the tensile strain had decreased along with the lateral deformation, leading to degradation in lateral resistance.

### 3.4 Residual deformation

Fig.8 shows the measured residual drift angles of all specimens. No significant difference was observed in the measured residual deformation among specimens with SBPDN rebars and USD rebars until  $R=0.025\text{rad.}$  Then the residual displacement of specimen FANUS gradually became larger than that of specimen FANSB. After the cover concrete of specimen FANSB seriously spalled off, the residual drift angle abruptly increased because the longitudinal rebar yielded and shear failure happened after  $R=0.04\text{rad.}$  The similar phenomenon can be seen when comparing the residual deformation of specimen FATUS with that of specimen FATSB. The residual drift angle of specimen FATSB gradually became smaller than that of specimen FATUS after  $R$  reached  $0.025\text{rad.}$  Therefore, one can say that the specimens with SBPDN rebars have smaller residual displacement than the specimen with USD rebars.

Until  $R$  is  $0.025\text{rad.}$  the residual deformation of specimens FANUS and FATUS were approximately the same, and the residual drift angle of specimen FANUS increased faster than that of specimen FATUS after that

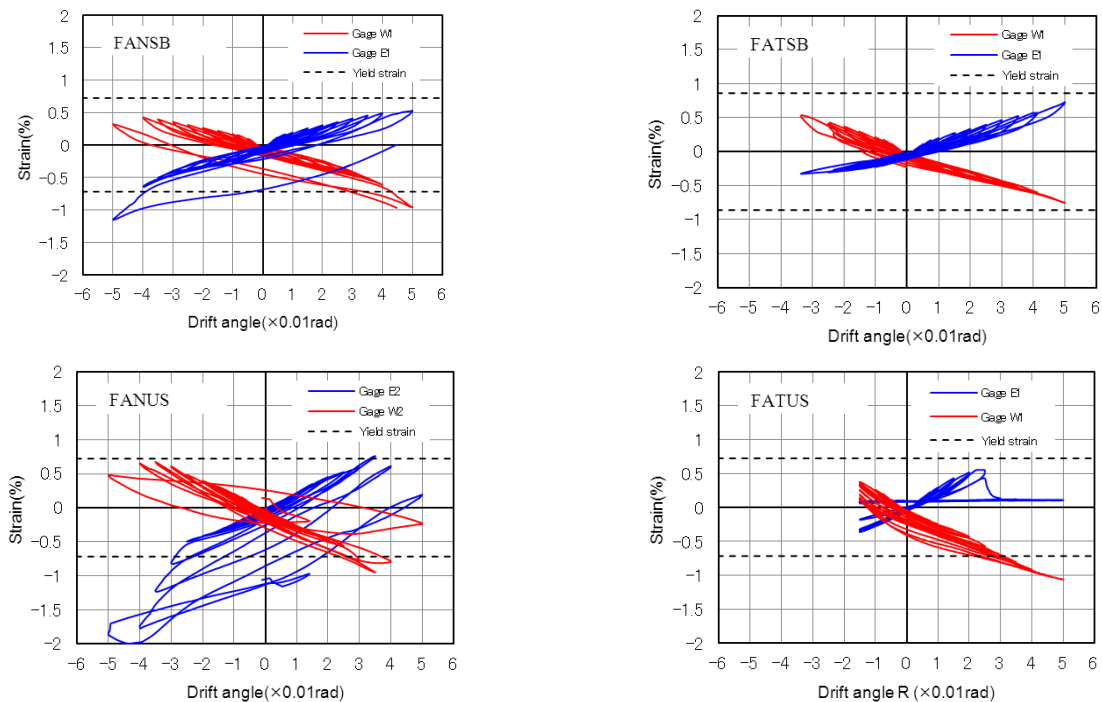


Fig. 7 The strain of longitudinal rebar

drift angle. Meanwhile, before R reached 0.05rad., the residual deformation of specimen FANSB had been a little larger than that of specimen FATSb, then the residual deformation of specimen FANSB gradually became larger. Therefore, it's reasonable to consider that specimens confined by steel plates have less residual deformation than specimens confined by conventional spirals at larger deformation.

We can find the reason by analyzing the largest strain of longitudinal rebar shown in Fig.7. When R reached 0.03rad., the strain of USD rebars in specimen FANUS exceeded its yield strain in tension, then shear failure occurred, which led to sharp increment in the residual deformation.

However, while the longitudinal rebar of specimen FATUS also started to yield when R reached 0.035rad., the residual deformation was still smaller than that of specimen FANUS due to higher and more effective confinement by the steel plates.

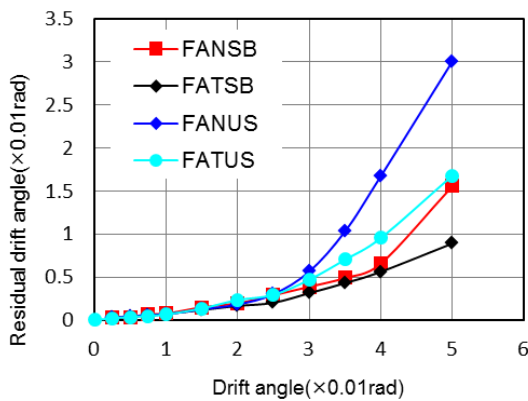


Fig.8 Residual displacement

#### 4 CONCLUSIONS

Four circular concrete columns were tested to investigate effects of combination of a large quantity of fine fly-ash, ultra-high-strength rebar with low bond strength, and confinement by thin steel plate, on seismic behavior of concrete columns. From the experimental results described in this paper, the following conclusion can be drawn.

- (1) Combination of a large quantity of fine fly-ash, ultra-high-strength rebar with low bond strength, and confinement by thin steel plate is a simple and effective method to create resilient concrete components. The concrete columns made of SBPDN rebars showed very stable seismic behavior till drift angle reached 0.05rad. without degradation in lateral resistance.
- (2) Residual displacements of specimens with SBPDN rebars were smaller than that of specimens with USD rebars, exhibiting higher resilience.

Specimens confined by steel plates have less residual displacement as compared to specimens confined by spirals after longitudinal rebar yielded at large deformation.

- (3) The damage of specimens with USD rebars was slighter in early loading stage, but became more serious in later loading stage as compared to specimens with SBPDN rebars. Specimens confined by steel plates showed much more subtle damage than the specimens confined by conventional spirals.
- (4) The residual deformation of concrete columns was mainly dependent upon whether the longitudinal rebar yielded or not rather than spalling off of the concrete shell.

#### ACKNOWLEDGMENTS

The ultra-high strength rebars were provided by Neturen Co. Ltd and Tokyo Rope MFG. Co. Ltd. The experimental investigation presented in this paper was jointly accomplished with Miss Yuka AONO and Mr. Kazuyuki SHIBATA, and also got help from Mr. Masaru KANAO when the columns were prepared and tested. The support received from them is gratefully acknowledged.

#### REFERENCES

- [1] Matsufuji Y, Koyama T, Ito K, "Mix Proportion Theory of Strength Controlling Concrete Containing Large Quantity of Coal Ash," Journal of the Society of Materials Science, Vol.51, No.10, 2002, pp.1111-1116.
- [2] Koyama T, Sun YP, Koyamada H, Fujinaga T, "Modeling of stress-strain relationship of concrete made with a large amount of fly-ash," Proceedings of the Japan Concrete Institute, Vol.30, No.3, 2008, pp.85-90.
- [3] Nakai S, Sun YP, Takeuchi T, Fujinaga T, "Seismic Performance of Concrete Column with High-Strength Reinforcing Bar Having Spiral Grooves," Proceedings of the Japan Concrete Institute, Vol.34, No.2, 2012, pp.163-168.
- [4] Sun YP, Sakino K, Yoshioka, T, "Flexural Behavior of High Strength RC Columns Confined by Rectilinear Reinforcement," Journal of Structural and Construction Engineering, Architectural Institute of Japan, No.486, 1996, pp.95-104.